Deciphering the kinetic structure of multi-ion plasma shocks

Brett D. Keenan, Andrei N. Simakov, Luis Chacón, and William T. Taitano

Phys. Rev. E **96**, 053203 — Published 15 November 2017

DOI: 10.1103/PhysRevE.96.053203

Deciphering the Kinetic Structure of Multi-Ion Plasma Shocks

Brett D. Keenan,* Andrei N. Simakov, Luis Chacón, and William T. Taitano
Los Alamos National Laboratory, Los Alamos, New Mexico 87545, USA

Strong collisional shocks in multi-ion plasmas are featured in many high-energy-density environments, including Inertial Confinement Fusion (ICF) implosions. However, their basic structure and its dependence on key parameters (e.g., the Mach number and the plasma ion composition) are poorly understood, and inconsistencies in that regard remain in the literature. In particular, the shock width's dependence on the Mach number has been hotly debated for decades. Using a high-fidelity Vlasov-Fokker-Planck code, iFP, and direct comparisons to multi-ion hydrodynamic simulations and semi-analytic predictions, we resolve the structure of steady-state planar shocks in D-^{3}He plasmas. Additionally, we derive and confirm with kinetic simulations, for the first time, a quantitative description of the dependence of the shock width on the Mach number and initial ion concentration.

I. INTRODUCTION

Strong shocks in multi-ion plasmas are key to a number of high-energy density settings. One prominent example is laser driven Inertial Confinement Fusion (ICF) implosions, which rely upon strong shocks for initial compression and heating of the fuel. It follows that multi-ion and kinetic effects associated with shocks may crucially affect the performance of ICF implosions [1–5]. ICF implosions, for example, are normally simulated with radiation-hydrodynamics (rad-hydro). Such a treatment is only valid for $N_K \ll 1$, where N_K (the Knudsen number) is the ratio of the constituent ions' mean-free-path to a characteristic gradient length scale. From simple hydro estimates, as the Mach number, M, of a collisional shock increases, so should N_K [6]. Consequently, the hydrodynamic treatment is formally valid for weak shocks with $M - 1 \ll 1$ [7, 8], where $N_K \sim 2(M - 1)$. Thus, a kinetic treatment is required for strong or intermediate-strength shocks. Despite this limitation, the structure of steady-state planar shocks in single species plasmas has been studied in the hydro limit by multiple authors [7, 9–11].

Initial kinetic studies of strong shocks in a single-species plasma employed the Mott-Smith ansatz. The Mott-Smith approach [12] admitted a solution to the Vlasov-Fokker-Planck (VFP) equations, by assuming that the particle velocity space distribution in a strong shock has a bi-Maxwellian form determined by the upstream and downstream conditions. These studies concluded that the kinetic shock width is considerably greater than the hydro equivalent [8, 12, 13], and is expected to grow with M [12, 14, 15]. Using a finite electron thermal conductivity, Ref. [12] predicted finite asymptotic growth and saturation of the ion shock width (normalized to a downstream mean-free-path) as $M \to \infty$. This broadening of the shock width for $M \gg 1$ was later observed in FPION VFP simulations of a hydrogen plasma shock [16, 17].

In contrast to the Mott-Smith prediction in Ref. [12], researchers using the hybrid Particle-in-Cell (PIC) code LSP found that the shock width (normalized to the ion-ion mean-free-path in the downstream) reaches a maximum at $M \sim 6$, and monotonically decreases for larger M [18].

It is worth noting that these studies typically considered single-ion plasmas. Hence, the structure of a collisional shock in a multi-ion plasma is a largely unexplored problem, and some peculiarities exist in the sparse multi-ion literature so far [18–20]. For example, FPION simulations for multi-ion (planar) plasma shocks in an equimolar mixture of deuterium and helium-3 [20] predicted deuterium temperature profiles overcoming electron temperature ones in the entirety of the electron pre-heat layer. Such a peculiar behavior was excused by the presence of ion kinetic effects.

However, as discussed in Ref. [6] using gas-kinetic arguments, the electron temperature is expected to exceed the temperature of all the ion species in the upstream portion of the pre-heat layer. This is due to the corresponding heat fluxes (plus the electron-ion energy exchange for the ions) being the main heating mechanisms for the species in this region; and the electron heat flux exceeding the ion heat flux by a factor of order $\sqrt{m_i/m_e} \gg 1$ (for low-Z ions) with m_e and m_i the electron and ion masses, respectively. This was found to be the case in earlier single ion-species FPION studies [17], as well as multi-fluid analyses [21].

The lack of consistency between the results of Ref. [17] and Ref. [20], both using the FPION code, appears even more puzzling once it is realized that the presence of ^{3}He in any D-^{3}He mixture render deuterons more collisional than in pure deuterium (or hydro-equivalent pure proton plasma which have the same ion-ion mean-free-path as pure deuterons; here, hydro-equivalence means the same mass density and pressure), and increased collisionality is expected to suppress kinetic effects.

In this work, we resolve these inconsistencies by systematically studying shocks in D-^{3}He plasma with a state-of-the-art VFP code, iFP. This code is fully mass, energy, and momentum conserving; it is also adaptive and well verified [23–27]. iFP treats ions fully kinetically, resolving both species within their own separate velocity-spaces, while simultaneously solving the quasi-neutral fluid equations for electrons [28].

For comparison, we also consider a multi-ion hydro description that is grounded in a multi-species generalization of the Braginskii equations [22, 28–30]. We note that a full multi-fluid formulation has not been available until recently. The analytic theory of multi-ion (hydro) plasma shocks employed in this paper is described in detail in Ref. [22]. This

* keenan@lanl.gov

theory is the first to include multi-ion physics, such as full ion diffusion. It does not, however, allow for temperature separation between ion species, since ion temperature separation is a higher-order effect in $N_K \ll 1$ (for details, see Ref. [22]). The hydro code has been benchmarked against analytical shock profiles for $M - 1 \ll 1$ [22].

The paper is organized as follows. Section II discusses intermediate-strength shocks ($M \gtrsim 1$) and Section III explores the strong shock ($M \gg 1$) regime. Section IV studies how the shock width changes with increasing Mach number, and presents the semi-analytic theory that underlies the shock width's dependence on M. Finally, we conclude in Section V.

II. INTERMEDIATE STRENGTH SHOCKS

Weak shocks are accurately described with multi-ion hydrodynamics [22]. We begin by demonstrating that iFP produces correct results in this limit. Recovering the hydro limit is difficult for Fokker-Planck codes, and therefore, this is a challenging verification test for iFP. In Fig. 1, we show electron and ion temperature comparisons between iFP and the multi-ion hydro results. The upstream mass concentration of deuterium (i.e., on the left side of the figure) is $c_0 \equiv m_D n_{D0}/\rho_0 = 0.57$, where m_D, n_{D0}, and ρ_0 are the deuterium mass, number density, and the total plasma mass density, respectively. The x-axis is normalized to the DD mean-free-path in the downstream, λ_{DD}^{DS}, and T_0 is the upstream temperature. Although an $M = 1.5$ shock is not strictly "weak", iFP and our multi-component hydro code demonstrate superb agreement. Note that, herein, all iFP and hydrodynamic simulations assume a constant Coulomb logarithm of 10 for all species.

In Fig. 2, we confirm very good agreement in the change of D concentration across the shock front between iFP and the multi-ion hydro simulation prediction for $M = 1.5$. Since the change in the deuterium mass concentration ($c - c_0$, where c_0 is the upstream concentration) is more sensitive to N_K than the temperatures [22], larger differences between the hydro and kinetic results are appreciated.

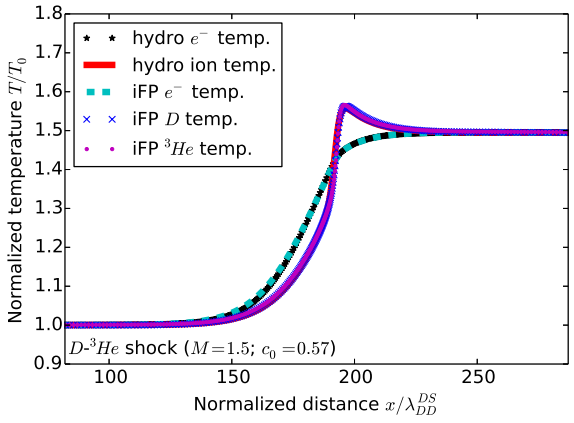

Figure 1: (Color online). Electron and ion temperature profiles for an $M = 1.5$ shock.

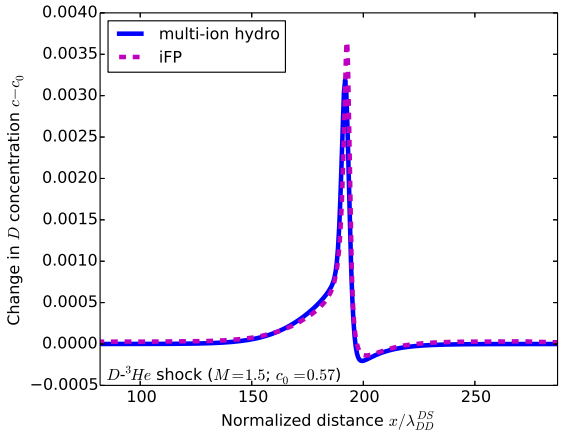

Figure 2: (Color online). Change in deuterium concentration, $c - c_0$, for an $M = 1.5$ shock.

III. STRONG SHOCKS

Next, we consider strong shocks. The structure of a strong (hydro) plasma shock is well known [7, 9–11], and is displayed in Fig. 3. There are three principal regions: 1) an electron pre-heat "pedestal" region where the electron temperature far exceeds the ion temperature, 2) the embedded/-compression ion shock, and 3) an equilibration layer where the electrons and ions relax to the downstream temperature. Both regions 1) and 3) are $\sim \sqrt{\frac{m_i}{m_e}}\lambda_{ii}$ (where m_i and m_e are the ion and electron masses, respectively, and λ_{ii} is the ion-ion downstream mean-free-path); whereas 2) is a few ion-ion mean-free-paths (mfps).

In the following plots, we feature an $M = 5$ D-^{3}He shock, since our simulations indicate that the essential structure of a plasma kinetic shock is adequately captured here (i.e., our results for higher M are qualitatively similar).

Figure 4 shows a considerable kinetic enhancement of the ion temperature in the pre-heat layer and at the shock front vs. the hydro simulations. Moreover, the D temperature is higher than the ^{3}He temperature in pre-heat layer, as expected from the lighter species. The deuterons also penetrate a greater depth into the upstream than ^{3}He due to the deuterons higher thermal velocity, as evidenced by Fig. 5. In contrast, the multi-component hydro result shows a sharp cutoff of the ion enrichment at the shock front, corresponding to a sharp gradient in the ion temperature. Consequently, the build up of deuterium in the upstream is a purely kinetic effect resulting from enhanced D ion mobility.

Lastly, it is worth examining the Knudsen numbers for all plasma species across the shock front. In Fig. 6, we have plotted $N_K \equiv \lambda_s \nabla \ln(T_s)$, where λ_s is the total mfp (i.e., in-

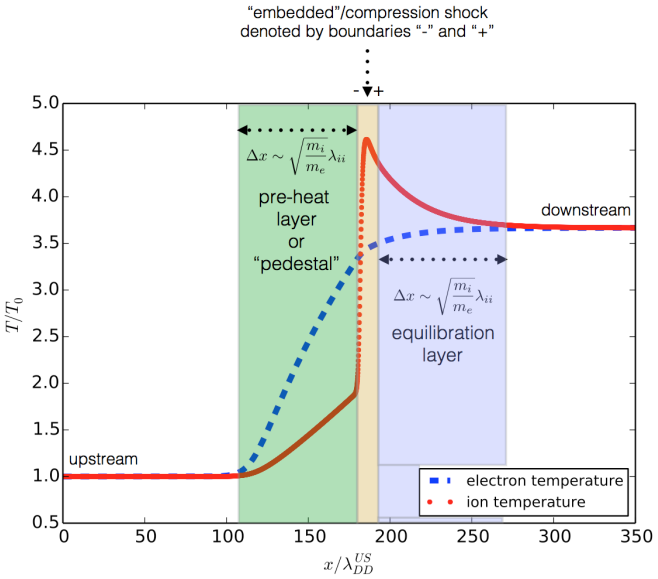

Figure 3: (Color online). Normalized temperature profiles for a hydro plasma shock with $M \gg 1$. T_0 is the upstream temperature.

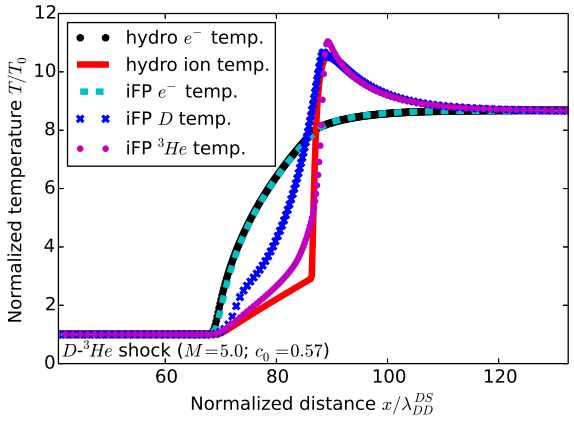

Figure 4: (Color online). Temperature profiles for an $M = 5$ shock.

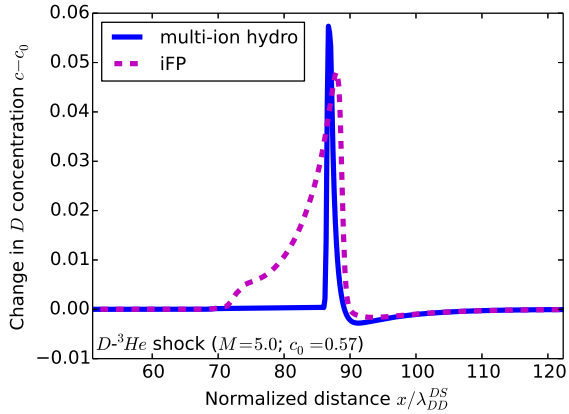

Figure 5: (Color online). Deuterium enrichment for an $M = 5$ shock.

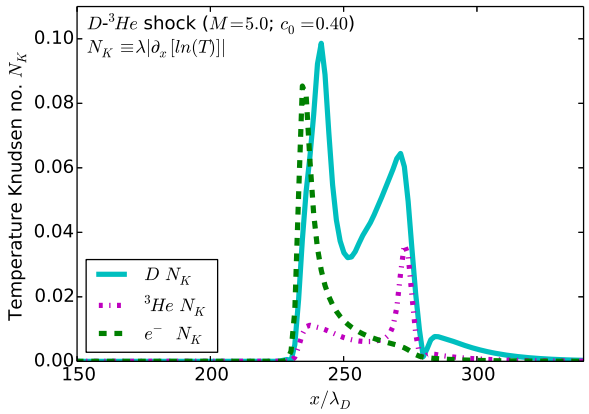

Figure 6: (Color online). Knudsen numbers for electrons, deuterons, and helium ions in an $M = 5$ planar shock in a 50-50% D-^{3}He plasma mixture. The x-axis is normalized to the total deuteron mean-free-path.

cluding interactions with all species) of species, s (i.e., for electrons, deuterium, and helium ions). Notice that the deuterium N_K approaches $\mathcal{O}(0.1)$ within the vicinity of the ion temperature pedestal's endpoints. This is to be expected, since these are the sites of the strongest temperature/density gradients in the hydro shock. The helium N_K is smaller than the deuterium N_K due to the higher collisionality (higher charge) of the former. Also note that the electron Knudsen number approaches $\mathcal{O}(0.1)$ at the leading edge of the pre-heat layer, indicating strong kinetic behavior, and the need to model electrons kinetically in this region.

IV. SHOCK WIDTH

As mentioned previously, various contradictory claims exist in the literature about the width of a plasma shock for $M \gg 1$. Here, we revisit this issue both from a fluid and a kinetic perspective, both of which are new. We begin by developing a semi-analytic fluid theory that describes the shock width as a function of M and c_0. As we will show later in this paper, the kinetic shock width behaves similarly to the hydro shock width, but with a quantifiable kinetic enhancement.

From Ref. [22], a hydrodynamic two-ion, steady-state, plasma shock may be described by two equations. Firstly, we have the electron energy equation:

$$\partial_{\hat{x}}\left(\frac{3}{2}\hat{p}_{e0}\hat{T}_e - \hat{\kappa}_e\partial_{\hat{x}}\hat{T}_e\right) + \hat{p}_{e0}\frac{\hat{T}_e}{\hat{V}}\partial_{\hat{x}}\hat{V} = \hat{\nu}_{ei}\left(\hat{T}_i - \hat{T}_e\right), \tag{1}$$

where $\hat{V} \equiv \rho_0/\rho$, $\hat{p}_{e0}$ is the electron pressure in the upstream normalized by the total upstream pressure, $\hat{\kappa}_e$ is the normalized electron thermal conductivity coefficient, $\hat{T}_i$ is the single ion temperature, $\hat{\nu}_{ei}$ is an electron-ion energy exchange frequency, $\hat{x}$ is the distance normalized to the DD mean-free-path in the upstream, and all other quantities are normalized to their respective upstream values. Next, we have an equation

for the ion mass density:

$$2\gamma M^2\left(\hat{V}-1\right)\left(\hat{V}_1-\hat{V}\right)+\frac{3}{2}\hat{\eta}\hat{V}\partial_{\hat{x}}\hat{V}\approx\hat{\kappa}_e\partial_{\hat{x}}\hat{T}_e, \quad (2)$$

where $\hat{\eta}$ is the normalized ion viscosity coefficient, $\hat{V}_1 \equiv \rho_0/\rho_1$, and $\gamma = 5/3$ is the adiabatic index.

The electron and ion temperatures inside the shock front scale as M^2, since they are of order the downstream temperature. Next, we note that $\hat{\nu}_{ei}(\hat{T}_i - \hat{T}_e)$ in Eq. (1) scales as $1/M^2$, since $\hat{\nu}_{ei} \propto M^{-4}$. This expression is generally smaller than the left-hand-side of the equation, owing to the fact that $\hat{\nu}_{ei}$ contains a factor of $\sqrt{\frac{m_e}{m_D}}$ and the energy exchange between ions and electrons is not the primary heating mechanism within the embedded shock. For this reason, we ignore the energy exchange term in Eq. (1), to obtain:

$$\left[\frac{3}{2}+\ln(\hat{V})\right]\hat{p}_{e0}\hat{T}_{e-}-\hat{\kappa}_e\partial_{\hat{x}}\hat{T}_e\approx const, \quad (3)$$

where we have used the fact that the electron temperature within the shock, denoted by $\hat{T}_{e-}$, is approximately constant [9]. The integration constant is effectively zero, as follows from the upstream boundary condition. Additionally, $1/4 \le \hat{V} \le 1$. Given these considerations, and the fact that $\hat{T}_{e-} \propto M^2$, we conclude that $\hat{\kappa}_e\partial_{\hat{x}}\hat{T}_e$ must also scale as M^2.

We now turn our attention to Eq. (2). The coefficient of ion viscosity, $\hat{\eta}$, scales as M^6. We may re-write Eq. (2) as:

$$\frac{d\hat{x}}{d\hat{V}}\approx\frac{\frac{3}{2}\hat{\eta}\hat{V}}{\hat{\kappa}_e\partial_{\hat{x}}\hat{T}_e-2\gamma M^2(\hat{V}-1)(\hat{V}_1-\hat{V})}, \quad (4)$$

from which we may conclude that $d\hat{x}/d\hat{V}$ scales as M^4, which is the Mach number dependence found in Refs. [13, 14] for strong shocks using the Mott-Smith ansatz. Reference [18] defined the shock width (S_W) as the length over which the ion density increases from 1.2 times its upstream value, ρ_0, to 0.9 times its downstream value, ρ_1 (normalized to the ion-ion mean-free-path in the downstream). For a meaningful comparison, we adopt the same definition. Normalizing to the downstream mfp introduces a factor of $1/M^4$, indicating that the normalized shock width:

$$S_W\equiv\frac{1}{\hat{V}_1\hat{T}_1^2}\int_{\hat{V}=\frac{1}{1.2}}^{\hat{V}=\frac{\hat{V}_1}{0.9}}\frac{d\hat{x}}{d\hat{V}}d\hat{V}, \quad (5)$$

does not scale with M, and therefore reaches a finite asymptotic value as $M \to \infty$, which is in agreement with Ref. [12].

To integrate this equation, we first note that the electron temperature within the embedded shock is approximately constant. For the portion of the pre-heat layer nearest to the upstream, $\ln(\hat{V}) \approx \hat{\nu}_{ei}(\hat{T}_i - \hat{T}_e) \approx 0$, and thus we may directly obtain the electron temperature in the pre-heat layer from Eq. (1) as [6]:

$$\hat{T}_e(\hat{x})\approx\left[\frac{15}{4}\frac{\hat{p}_{e0}}{\hat{\kappa}_{e0}}(\hat{x}-\hat{x}_0)+1\right]^{\frac{2}{5}}, \quad (6)$$

where $\hat{\kappa}_{e0} \equiv \hat{\kappa}_e|_{\hat{x}=\hat{x}_0}$, and $\hat{x}_0$ is the position of the upstream edge of the pre-heat layer. To obtain $\hat{T}_{e-}$, we evaluate Eq. (6) at the location of the embedded shock, which is at $\hat{x} - \hat{x}_0 = \hat{x}^{pre-heat} \sim \lambda_{ee}v_{the}/(u_0\lambda_{DD}^{US})$, where λ_{DD}^{US} is the ion-ion mean-free-path in the upstream, and u_0 is the shock velocity. It is easy to show that $x_{pre-heat} \sim \sqrt{\frac{m_i}{m_e}}\lambda_{ii}^{DS} \sim \lambda_{ee}\frac{v_{the}}{u_0}$. The exact value of $\hat{x}^{pre-heat}$, which depends on c_0, M, etc., is unknown. Consequently, we slightly tweak $\hat{T}_{e-}$ to best fit the results from full multi-ion hydro simulations. An expression for $\hat{T}_{e-}$ allows us to estimate [22] $\hat{\eta} \propto \hat{T}_i^{5/2}$, where $\hat{T}_i$ is given by the expression:

$$\hat{T}_i\approx f(c_0,\mu,\xi)\left[1-\gamma M^2\left(\hat{V}-1\right)\right]\hat{V}-[f(c_0,\mu,\xi)-1]\hat{T}_{e-}. \quad (7)$$

with $\mu \equiv m_2/m_1$ and $\xi \equiv Z_2/Z_1$, being the ion mass and charge ratios, respectively.

The final step is to obtain an expression for $\hat{\kappa}_e\partial_{\hat{x}}\hat{T}_e$ within the embedded shock. Our hydro simulations indicate that the ion viscosity is only important near the middle of this domain. Consequently, Eqs. (2)–(3), imply:

$$\hat{\kappa}_e\partial_{\hat{x}}\hat{T}_e\approx 2\gamma M^2\left(\hat{V}_- -1\right)\left(\hat{V}_1-\hat{V}_-\right)+\hat{p}_{e0}\hat{T}_{e-}\ln\left(\frac{\hat{V}}{\hat{V}_-}\right), \quad (8)$$

where $\hat{V}_- = 1/1.2$, as per our definition of the shock width. Our simulations have confirmed that this is a decent approximation.

Now, with Eqs. (4)–(8), we may obtain the hydro shock width as a function of M and c_0.

Figure 7, depicts for $M = 5$ as a function of c_0. The semi-analytic curve for $M = 5$, the (blue) "dashed" line, matches the multi-ion hydro simulation points, shown in (red) "stars", fairly closely. To show the full dependence of S_W on c_0, we have normalized S_W to $\lambda_D^{DS} \equiv 1/(\lambda_{DD}^{-1} + \lambda_{D^3He}^{-1})$.

Figure 8 shows the shock width as a function of Mach number from full multi-ion hydro simulations as (red) "stars" for $c_0 = 0.40$, along with a gray dashed fit curve. The figure also shows the corresponding iFP shock width. Overlapping the latter points is the fit for the hydro regime, translated upward by a fixed amount that depends on c_0, but not M. We see that the kinetic shock width, for $M \gg 1$, is simply the multi-ion hydro shock width plus a correction. It follows that the kinetic shock width also asymptotes to a constant as $M \to \infty$. This result consistent with the Mott-Smith results from Refs. [12–14], but is at odds with Ref. [18], which predicted that the shock width decreases for $M \gtrsim 6$.

The kinetic extension of the shock width is simply due to hot downstream ions penetrating upstream beyond the ion density pedestal [13, 17]. We may quantify this effect by plotting the kinetic shock width enhancement, $S_W^{iFP} - S_W^{hydro}$, vs. c_0, normalized to the length of the electron pre-heat layer (as in Fig. 9). Note that the S_W enhancement is independent of M. In Fig. 9, the dots are from simulations, and the (green) "dashed" line is a characteristic ion energy relaxation distance.

The ion energy relaxation distance is obtained by considering a flow of downstream deuterons into a colder pedestal

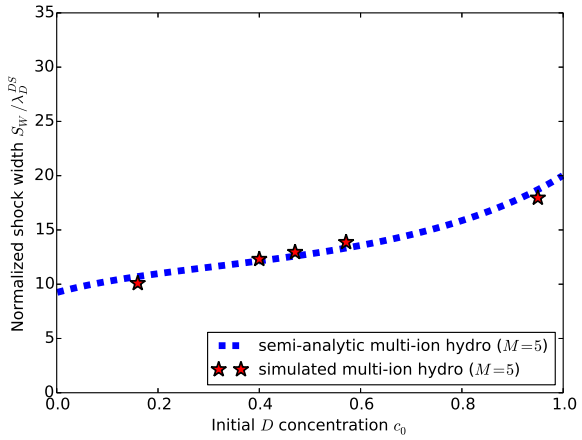

Figure 7: (Color online). Semi-analytic multi-ion hydro shock width (for $M = 5$) vs. c_0. Included are results from full multi-ion hydro simulations.

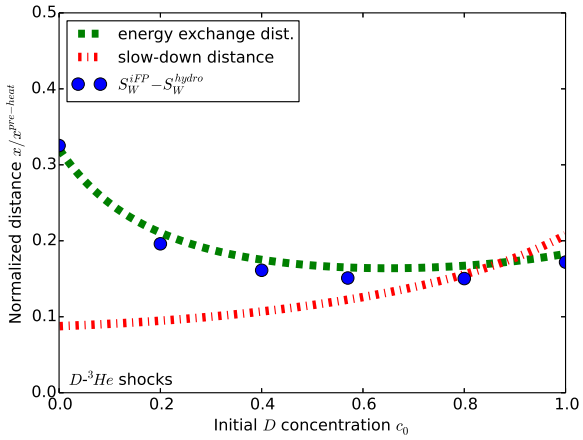

Figure 9: (Color online). $S_W^{iFP} - S_W^{hydro}$ normalized to the length of electron pre-heat layer vs. c_0 with two proposed theoretical models.

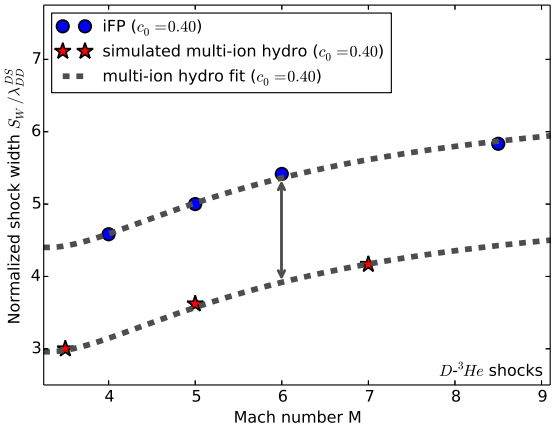

Figure 8: (Color online). The ion shock width vs. Mach number for $M = 5$ and $c_0 = 0.40$.

plasma in the upstream. Kinetic effects are most prominent in the pedestal, since this is the site of the sharpest gradients in temperature, density, etc. Additionally, this definition of the distance is independent of Mach number for $M \gg 1$ [11].

This distance can be estimated by considering a characteristic time for hot particles, α, to exchange energy with colder background plasma particles, β [31], given by: $(\tau_\epsilon^\alpha)^{-1} \equiv \sum_\beta 1/\tau_\epsilon^{\alpha/\beta}$, where $\tau_\epsilon^{\alpha/\beta} \equiv \frac{\tau_1^{\alpha/\beta}}{4\mu(x_\beta)/x_\beta}$, $x_\beta = \left(\frac{m_\beta}{m_\alpha}\right)\frac{T_\alpha}{T_\beta}$, $\mu(x) = \frac{2}{\sqrt{\pi}}\int_0^x \sqrt{t}e^{-t}dt$, $\tau_1^{\alpha/\beta} = \frac{\sqrt{m_\alpha}}{\pi\sqrt{2}e_\alpha^2 e_\beta^2}\frac{T_\alpha^{3/2}}{n_\beta \ln(\Lambda)}$, with $\ln(\Lambda)$ the Coulomb logarithm, T_α the downstream D temperature, n_β and T_β the number densities and temperatures of the plasma species in the pedestal region, respectively, and m_α, m_β, e_α, and e_β the corresponding masses and charges. The ion energy relaxation distance for D is defined in terms of the shock velocity, u_0 as:

$$d_\epsilon \equiv u_0 \tau_\epsilon^D. \tag{9}$$

The agreement between the numerical kinetic S_W enhancement and this ion energy relaxation distance in Fig. 9 is remarkable.

Figure 9 also depicts the characteristic slowing-down distance (red) "dash-dotted" line, proposed in Ref. [17] as an alternate measure of the kinetic extension of a plasma shock the slowing-down distance, which is defined similarly to that in Eq. (9), but in terms of the slow-down time: $\tau_s^{\alpha/\beta} \equiv \tau_1^{\alpha/\beta}/\left[\left(1+\frac{m_\alpha}{m_\beta}\right)\mu(x_\beta)\right]$ [31].

Evidently, the extension of the kinetic shock width is more accurately represented by the total ion energy relaxation distance than by the slowing-down distance. Figure 9 makes one final important point, namely, that the ion energy exchange distance is smaller than the electron pre-heat layer width for all c_0, confirming that the ion temperature does not overcome the electron temperature in the upstream edge of the pre-heat layer.

V. DISCUSSION

In conclusion, this work has unravelled the rich structure of multi-ion plasma shocks. We began by demonstrating that our kinetic code, iFP, is capable of accurately resolving the weak shock regime. This is the hardest regime for VFP codes, and the iFP results show excellent agreement with multi-ion hydro simulations, underscoring IFP's accuracy and reliability.

Next, we examined the strong shock regime. For an $M = 5$ shock in D-^{3}He, we showed that the kinetic shock structure markedly differs from multi-ion hydro predictions. This was most apparent in the enhanced abundance of deuterium ions

in the pre-heat layer of the shock, which is solely a kinetic effect.

Additionally, we found that kinetic effects saturate for $M \gg 1$ (i.e., the kinetic extension of the shock width, normalized to a downstream mean-free-path, becomes independent of the Mach number). Moreover, the asymptotic value strongly depends on the upstream lighter species concentration. This is true of both the multi-ion hydro and kinetic shock widths, with the latter exceeding the former by a characteristic ion energy exchange distance. Our findings, while consistent with early Mott-Smith predictions [12] and Fokker-Planck results [17], conflict with the LSP (PIC) predictions from Ref. [18]. Given the outstanding agreement between iFP and our theoretical predictions, we believe that the debate over the shock width's dependence on M may now be safely laid to rest.

Lastly, we confirmed that the ion temperature never exceeds the electron temperature in the pre-heat layer, contradicting a recent study with FPION [20], but in agreement with an earlier FPION study [17], and a study using a multi-fluid model [21]. Rather, we found that the kinetic multi-ion shock width, which is a proxy for the ion temperature, is extended beyond the hydro one by a characteristic energy exchange distance, which is smaller than the length of the electron pre-heat layer.

This result is physically grounded. The basic argument is as follows. The heat flux for species, s can be estimateed by $q_i \sim p_s v_{th,s} \min(N_K^s, FL_s)$ with p_s, $v_{th,s} = \sqrt{2T_s/m_s}$, N_K^s, and FL_s the pressure, thermal speed, Knudsen number, and flux limiter, respectively. This expression is applicable for all N_K^s, and therefore, for all M. We do not expect the electron and ion flux limiters to be drastically different in the kinetic regime ($FL_e = 0.05$-0.15 is typically used in ICF rad-hydro simulations [32]). Additionally, we showed in Fig. 6 that the ions and electrons have comparable Knudsen numbers throughout the pre-heat layer. Since ions and electrons have comparable temperatures immediately upstream of the compression shock (i.e., the roughly defined boundary between the compression shock and the pre-heat layer). The ratio of the electron to deuteron heat fluxes (for D-^{3}He with $c_0 = 0.40$, as a concrete example), therefore, becomes:

$$\frac{q_e}{q_i} \sim \frac{p_e v_{th,e} \min(N_K^e, FL_e)}{p_D v_{th,D} \min(N_K^D, FL_D)} \sim 3\sqrt{\frac{m_D}{m_e}} \sim 182, \quad (10)$$

where we have used $FL_i = 1.0$, $FL_e = 0.1$, and $N_K^e = N_K^i = 0.1$ (valid for $M \gg 1$). Thus, the electron heat flux is much larger than the deuteron (or ^{3}He) heat flux at the beginning of the pre-heat layer (which is then carried throughout the layer, as the electron temperature gradient becomes sharper and sharper), resulting in higher electron temperatures.

Finally, as mentioned previously, Fig. 6 speaks to the need for a kinetic treatment for the electrons, since N_K^e becomes quite large near the upstream end of the pre-heat layer. This is to be expected, since the electron temperature exhibits a very sharp gradient there. Hence, the true kinetic structure of collisional plasma shocks has yet to be explored, since kinetic electrons are likely important in the outer-edge of the pre-heat layer. Nevertheless, we do not expect electron kinetic effects to be important within the compression shock itself. Consequently, our results for the shock width should hold generally.

ACKNOWLEDGMENTS

Acknowledgments.–This work was supported by the Los Alamos National Laboratory LDRD Program, Metropolis Postdoctoral Fellowship for W.T.T., and used resources provided by the Los Alamos National Laboratory Institutional Computing Program. Work performed under the auspices of the U.S. Department of Energy National Nuclear Security Administration under Contract No. DE-AC52-06NA25396.

[1] H. G. Rinderknecht *et al.*, Phys. Rev. Lett. **114**, 025001 (2015).
[2] M. J. Rosenberg *et al.*, Phys. Rev. Lett. **112**, 185001 (2014).
[3] M. J. Rosenberg *et al.*, Phys. Plasmas **21**, 122712 (2014).
[4] H. G. Rinderknecht *et al.*, Phys. Rev. Lett. **112**, 135001 (2014).
[5] M. J. Rosenberg *et al.*, Phys. Plasmas **22**, 062702 (2015).
[6] Y. B. Zel'dovich and Y. P. Raizer, *Physics of shock waves and high-temperature hydrodynamic phenomena*, edited by W. D. Hayes and R. F. Probstein (Academic Press, New York, 1967), Vol. 2, pp. 515-520.
[7] J. D. Jukes, J. Fluid Mech. **3**, 275 (1957).
[8] H. M. Mott-Smith, Phys. Rev. **82**, 885 (1951).
[9] V. D. Shafranov, Soviet Phys. JETP **5** (1957).
[10] M. Y. Jaffrin and R. F. Probstein, Phys. Fluids **7**, 1658 (1964).
[11] M. S. Grewal, Phys. Fluids **16**, 561 (1973).
[12] M. S. Greywall, Phys. Fluids **18**, 1439 (1975).
[13] K. Abe, Phys. Fluids **18**, 1125 (1975).
[14] D. A. Tidman, Phys. Rev. **111**, 439 (1958).
[15] C. Muckenfuss, Phys. Fluids **3**, 320 (1960).
[16] M. Casanova, O. Larroche, and J. P. Matte, Phys. Rev. Lett. **67**, 2143 (1991).
[17] F. Vidal, J. P. Matte, M. Casanova, and O. Larroche, Phys. Fluids B **5**, 3182 (1993).
[18] C. Bellei *et al.*, Phys. Plasmas **21**, 056310 (2014).
[19] C. Bellei and P. A. Amendt, Phys. Rev. E **90**, 013101 (2014).
[20] O. Larroche, Phys. Plasmas **19**, 122706 (2012).
[21] S. I. Glazyrin, A. S. Kuratov, and V. Y. Bychenkov, Sov. Phys. JETP Lett. **103**, 238 (2016).
[22] A. N. Simakov, B. D. Keenan, W. T. Taitano, and L. Chacón, Phys. Plasmas **24**, 092702 (2017).
[23] W. T. Taitano, L. Chacón, and A. N. Simakov, J. Comput. Phys. **297**, 357 (2015).
[24] W. T. Taitano, L. Chacón, and A. N. Simakov, J. Comput. Phys. **318**, 391 (2016).
[25] L. Yin, B. J. Albright, W. Taitano, E. L. Vold, L. Chacón, and A. N. Simakov, Phys. Plasmas **23**, 112302 (2016).
[26] W. T. Taitano, L. Chacón, and A. N. Simakov, J. Comput. Phys. **339**, 453 (2017).
[27] W. T. Taitano, L. Chacón, and A. N. Simakov. "An adaptive, implicit, conservative 1D-2V multi-species Vlaslov-Fokker-Planck multiscale solver in planar geometry", submitted to J.

Comp. Phys. (2017).
[28] A. N. Simakov and K. Molvig, Phys. Plasmas **21**, 024503 (2014).
[29] A. N. Simakov and K. Molvig, Phys. Plasmas **23**, 032115 (2016).
[30] A. N. Simakov and K. Molvig, Phys. Plasmas **23**, 032116 (2016).
[31] B. A. Trubnikov, in *Reviews of Plasma Physics*, edited by M. A. Leontovich (Consultants Bureau, New York, 1965), Vol. 1, p. 105.
[32] A. N. Simakov, D. C. Wilson, S. A. Yi *et al.*, Phys. Plasmas **21**, 022701 (2014).